

Modelling the inflammatory response of traumatic brain injury using human induced pluripotent stem cell derived microglia

Aftab Alam*¹, Tanya Singh*², Saeed Kayhanian*¹, Jonathan Tjerkaski³, Núria Marcó Garcia¹, Keri L. Carpenter¹, Rickie Patanie⁴, Caroline Lindblad^{3,5,6}, Eric P.Thelin^{1,3,7},
Yasir Ahmed Syed**², Adel E. Helmy**¹

1. Department of Clinical Neurosciences, University of Cambridge, UK
2. School of Biosciences and Neuroscience and Mental Health Innovation Institute, Cardiff University, UK
3. Department of Clinical Neuroscience, Karolinska Institutet, Stockholm, Sweden
4. Institute of Neurology, Queen Square, University College London, UK
5. Department of Neurosurgery, Uppsala University Hospital, Uppsala, Sweden
6. Department of Medical Sciences, Uppsala University, Uppsala, Sweden
7. Department of Neurology, Karolinska University Hospital, Stockholm, Sweden

*Joint first authors

** Joint senior authors

Email addresses:

Aftab Alam	alam.camb@gmail.com
Tanya Singh	tanya.singh@ndcn.ox.ac.uk
Saeed Kayhanian	sk776@cam.ac.uk
Jonathan Tjerkaski	jonathan.tjerkaski@stud.ki.se
Núria Marcó Garcia	nuria.marcog@hotmail.com
Keri L. Carpenter	klc1000@icloud.com
Rickie Patanie	rickie.patani@ucl.ac.uk
Caroline Lindblad	caroline.lindblad@ki.se

Eric P.Thelin eric.thelin@ki.se

Yasir Ahmed Syed SyedY@cardiff.ac.uk

Adel E. Helmy aeh33@cam.ac.uk

Corresponding author:

Saeed Kayhanian

Department of Clinical Neurosciences

University of Cambridge

Cambridge Biomedical Campus

CB2 0QQ

sk776@cam.ac.uk

Abstract

The neuroinflammatory response after traumatic brain injury (TBI) is implicated as a key mediator of secondary injury in both the acute and chronic periods after primary injury. Microglia are the key innate immune cell in the central nervous system, responding to injury with the release of cytokines and chemokines. In this context, we aimed to characterise the downstream cytokine response of human induced pluripotent stem cell (iPSC)-derived microglia when stimulated with five separate cytokines identified following human TBI. iPSC-derived microglia were exposed to IL-1 β , IL-4, IL-6, IL-10 and TNF in the concentration ranges identified in clinical TBI studies. The downstream cytokine response was measured against a panel of 37 separate cytokines over a 72-hour time-course. The secretome revealed concentration-, time- and combined concentration and time-dependent downstream responses. TNF appeared to be the strongest inducer of downstream cytokine changes (51), followed by IL-1 β (26) and IL-4 (19). IL-10 (11) and IL-6 (10) produced fewer responses. We also compare these responses to our previous studies of iPSC-derived neuronal and astrocyte cultures and the in-vivo human TBI cytokine response. Notably, we found microglial culture to induce both a wider range of downstream cytokine responses and a greater fold change in concentration for those downstream responses, as compared to astrocyte and neuronal cultures. In summary, we present a dataset for human microglial cytokine responses specific to the secretome found in the clinical context of TBI. This reductionist approach complements our previous datasets for astrocyte and neuronal responses and will provide a platform to enable future studies to unravel the complex neuroinflammatory network activated after TBI.

Keywords: traumatic brain injury, neuroinflammation, inflammation, microglia, cytokine, microdialysis

Introduction

Traumatic brain injury (TBI) is a major public health concern, affecting around 30 million people worldwide each year^{1,2}. The treatment options for TBI remain limited and, in the absence of effective pharmacological neuro-protective strategies, current guidelines focus on limiting secondary injury through targeted correction of physiological parameters. It is known, however, that this secondary injury is mediated, at least in part, by an innate inflammatory response, mediated through the release of cytokines and chemokines that act in a dose- and time- dependent manner^{3,4}. The development of immunomodulatory therapies for TBI will require a detailed understanding of this complex neuroinflammatory response which is likely to have both beneficial and deleterious effects, at different time points, to the injured brain.

Microglia are the major cellular component of the innate immune system in the brain and are found in significant numbers throughout the brain, composing around 10% of all cells in the brain⁵. In response to injury, they are known to respond rapidly to accumulating Damage Associated Molecular Patterns (DAMPs) and chemokine signals in the local milieu of the brain, with a transformation to an “activated” state characterised by a morphological change from ramified to amoeboid cell structure⁶. These microglia respond to injury through the secretion of cytokines which signal to neurons and glia in the injured brain in a paracrine fashion. This response is complex, with microglia adopting multiple possible activation states and the downstream cytokine response complicated further signalling networks with glia and neurons^{7,8}.

In this context, we undertake a reductionist approach to discover the microglial component of the early cytokine response to TBI. Here we examine the response of human induced pluripotent stem cell (iPSC)-derived microglia to five cytokines at physiologically relevant concentrations that are found after TBI. The added cytokines are the most widely studied pro- (IL-1 β , IL-6, TNF) and anti-inflammatory (IL-4, IL-10) cytokines in the clinical TBI literature and the downstream cytokine generation was measured against a panel of 37 chemokine and cytokine responses. We compare these responses to our previous studies of iPSC-derived neuronal and astrocyte cultures and the in-vivo human TBI cytokine response.

Methods

Human induced Pluripotent Stem Cell-derived microglia

Human microglia were derived from human induced Pluripotent Stem Cells (iPSCs)⁹. In brief, iPSCs were grown on Geltrex™ coated plates in E8F media with media changed every 48 hours and were maintained between 30% and 80% confluency at 37°C and 5% CO₂. At 70% to 80% confluency iPSCs were passaged using Versene solution (Gibco™ 15040066) and gently triturated to form a suspension of uniform clumps. The clusters were then transferred to Corning ultra-low attachment 6-well plates with microglia differentiation media, MDM (supplemented with 10ng/mL IL-34 + 10ng/mL CSF1). Embryoid bodies (EBs) were monitored for 2 weeks. At day 14, the EBs were transferred on poly-D-lysine coated plates. For next 30 days (every 5th day), EBs were gently triturated, positively selected the single cells of interest and seeded on Primaria plates. The attached single cells on Primaria plate were maintained and checked for microglia like/microglial precursors like morphology. Further maintenance was performed in microglia maintenance media, MGM (supplemented with 100 ng mL⁻¹ IL-34 + 5 ng mL⁻¹ CSF1).

Cytokine induction

Human recombinant IL-1 β (#11457756001), IL-4 (#I4269), IL-6 (#I1395), IL-10 (#IL010), and TNF (#T6674) were each sourced as lyophilized powder (Merck, Kenilworth, NJ), which was reconstituted according to the manufacturer's instructions. Each of the five cytokines were diluted into three different concentrations and each culture well was further technically duplicated (i.e., two supernatants isolated per time point). This resulted in 45 experimental samples (2 technical repeats for each of 5 different inducing cytokine concentrations at 3 different time points), including the unstimulated samples collected at 0h considered to be the controls. The three cytokine concentrations (low, medium, high) were chosen to cover the range of concentrations seen in human microdialysis studies, adjusted for relative recovery determined in vivo (summarised in Table 1).

Sample collection and storage

Supernatant (60 μ L) was taken from each cell culture well at the given time points (0, 1, 24, 48, and 72h), including control lines (n = 2 technical repeats). The cells were collected at 1, 24, 48, and 72h following addition of the respective cytokine and from untreated cultures (n = 2 per time point). Samples were stored at -80°C until analysis.

Cytokine analysis

Each experimental condition/technical repeat was analysed in duplicate (i.e., two samples per experimental cell culture well). The supernatants were analysed using the Procartaplex 37-PLEX, Human Cytokine/Chemokine 37 (ThermoFisher, Waltham, MA) using the manufacturer's instructions as previously described, with overnight incubation. As described, the time points 0 (for control wells), 1, 24, 48, and 72h were analysed. The plates were analysed on a Luminex 200 platform (Luminex Corporation, Austin, TX). As per manufacturer's recommendation, cytokine concentrations were calculated by reference to an eight-point five-parameter logistical standard curve for each cytokine.

Immunocytochemistry

Cells were washed once with 1X PBS and then incubated with 4% paraformaldehyde for 15 minutes at room temperature. Paraformaldehyde was then removed, and cells were washed twice with 1X PBS. Cells were blocked for 1 hour and permeabilized using a 3% donkey serum prepared in 1X PBS with 0.03% Triton-X-100 (PBST). Primary antibodies: IBA1 (Wako, 019-19741), CD-40 (eBioscience, 14-0409-82), TNF-A (Novus, NBP119532), MAP2 (Abcam, AB32454) were then made up in the blocking solution and incubated overnight at 4 °C. The primary antibody solution was then removed, and cells were washed 3 times with 1X PBS. Secondary antibodies were diluted 1:1000 in PBST and applied for 1 hour at room temperature. The secondary antibody solution was then removed, and cells were washed twice with 1X PBS before counterstaining with DAPI and mounted using Fluoromount Mounting Medium (Sigma). Imaging was done on a Leica DMI600 Inverted Microscope.

Quantitative Real-Time PCR (qRT PCR)

RNA was isolated using a GeneElute mammalian total RNA miniprep kit (Sigma) according to the manufacturer's protocol. RNA was eluted in 20µl of nuclease-free water and the concentration of RNA was measured using a nano-drop machine. 500ng of RNA was then used to create cDNA using a high-capacity cDNA reverse transcription kit (Applied Biosystems) based on the manufacturer's protocol. 100ng of cDNA was used for 20 µl of qRT-PCR reaction performed on a StepOnePlus real-time PCR system (Applied Biosystems) with qPCR SyGreen Blue Mix Hi-ROX (PCR). Threshold cycle (CT) numbers were normalized to the expression of house-keeping gene, GAPDH. Fold change in gene expression is calculated by the $2^{-\Delta\Delta CT}$ method and relative mRNA abundance is calculated by $2^{-\Delta CT}$ method.

Phagocytosis

Cells were plated in a 96-well nunc plates and maintained in DMEM in advance of performing assays. The assay was performed according to the manufacturer's protocol (Vybrant™ Phagocytosis Assay Kit, V6694). The cells were incubated in DMEM and LPS (20 ng mL⁻¹) for 1 hour at 37 °C and 5% CO₂. The cells were then washed with DPBS and 100 µL of fluorescein-labeled *E. coli* BioParticles® suspended in Hanks' balanced salt solution was added and incubated further for 2 hours at 37 °C and 5% CO₂. The suspension was then aspirated, and 100 µL per well of trypan blue suspension was added for 1 min. After aspiration of trypan blue from the wells, the reading of the experimental and control wells of the microplate were measured using a fluorescence plate reader with appropriate sensitivity settings.

Clinical and in-vitro cytokine data

We extracted data from two previous studies from our group that measured cytokine concentrations from TBI patients who were monitored over 5 days, with cytokine samples pooled from 6-hour periods^{10,11}. All data was corrected to the time of injury to enable comparison with in-vitro data. Data was also extracted from our previous reductionist studies of downstream cytokine response to enriched neuronal and astrocyte cultures^{12,13}.

Similar to this study, the astrocyte samples were exposed to IL-1 β , IL-4, IL-6, IL-10, and TNF, while enriched neuronal cultures were exposed to IL-1 β , IL-6, and TNF only.

Statistical analysis

R was used to carry out the statistical analysis (Version 3.6.0, R Core Team, 2018). Two-way repeated measures analysis of variance (ANOVA) was used to assess the effect of each inducing cytokines on the secretion of cytokines by microglia, across different concentrations of the inducing cytokines and across time. The dependant variables in these analyses were the concentration of secreted cytokines, while the independent variables were the concentration of the inducing cytokine and time, with an interaction between the two independent variables. Pair-wise comparisons were made using Tukey's honestly significant difference (HSD) test. $p < 0.05$ was regarded as statistically significant.

Results

Morphology, gene expression and functional activity of iPSC-derived microglia

Microglia were derived using the previously published protocol, differentiated from the iPSC control line using multiple growth factors⁹. After 50 days of differentiation, the iPSC-derived microglia were associated with their characteristic morphology and were positive for the expression of microglial markers IBA1, CD40, and TNF-A (Figure 1A, 1B). These functional activity of these microglia was confirmed by phagocytosis assay following stimulation with LPS (Figure 1C). These microglia also showed expression of MMP2, MMP9, and IL-1B suggesting their competence to respond to cytokine stimulation.

Temporal and concentration dependent effects of added cytokines to microglial cultures

Stimulation of the microglial cultures with the five cytokines at physiologically relevant ranges led to the downstream production of cytokines, with both time- and concentration-dependent changes in the levels of these downstream cytokines in culture (Table 2 and Figure 2A). TNF appeared to be the strongest inducer of downstream cytokine changes (51 cytokine changes, $p < 0.05$), followed by IL-1 β (26 cytokines) and IL-4 (19 cytokines). IL-10 and IL-6 produced fewer responses (11 and 10 cytokines respectively).

Cytokine temporal patterns of microglia compared to in vivo and other cell types in vitro

We next compared the temporal profiles of cytokine release from microglia cultures in vitro to our previous in vivo and in vitro cytokine studies. Here we compared the patterns of time-resolved cytokine release in the brain extracellular fluid from TBI patients, as well as in vitro data from enriched neuronal cultures (exposed to IL-1 β , IL-6, and TNF) and astrocyte cultures (exposed to IL-1 β , IL-4, IL-6, IL-10, and TNF) (Figure 2B, 2C). A summary of the in vitro data is shown in Table 3.

We found that the in vitro secretome response of all three cell types followed broadly similar temporal trends with comparable mean concentrations of the downstream cytokines found in the supernatant (Figure 2B, 2C). The in vivo results trend towards a much faster response as well as higher overall concentrations of the downstream cytokines, even accounting for the summative effects of all three cell types being present.

Discussion

We present here a systematic study of the downstream cytokine signalling from human microglial cultures, stimulated with canonical pro- and anti-inflammatory cytokines. The stimulating cytokines were used at clinically relevant concentrations, derived from measurements in human TBI conditions. This is a key feature of our approach, compared with other studies in the literature which have utilised concentrations orders of magnitude higher. We characterised responses using a multiplex platform, examining the microglial secretome for 37 separate downstream cytokines and chemokines in parallel. This provides a powerful reference framework in a specifically human context, as compared to previous work that has either been done in mice or using only individual assays of a few downstream cytokines. This human context is particularly important for future translational work and the development potential therapies targeting neuro-inflammatory secondary injury, as translation from murine models in this context appears to have limited applicability.

The microglial secretome demonstrated in this study emphasises the role of microglia as the resident innate immune cell in the brain, with a downstream cytokine response that is both broader (in terms of number of separate cytokines released) and larger (in terms of fold-change in concentration), compared to our previous similar studies of human astrocyte and

neuronal cultures^{12,13}. Further, the putative pro- and anti-inflammatory distinction between added cytokines was not clearly apparent in downstream responses, with both IL-4 and IL-10 exhibiting dose-dependent stimulation of canonical pro-inflammatory cytokines such as IL-6, Interferon (IFN)- α , and IFN- γ . This mixed inflammatory profile from microglia has also been evidenced also in mouse models of TBI, where concurrent pro- and anti-inflammatory networks appear to be upregulated throughout acute and chronic (up to 60 days) periods after cortical injury^{8,14}. The pattern of any potential cytokine driving a further cytokine response in these cultures suggests microglia may be driven by a positive feedback loop in the injured microenvironment of the brain, in keeping with evidence of activated microglia throughout acute and chronic periods after brain injury¹⁵.

TNF appeared the most potent activator of downstream cytokine response in the microglial cultures, consistent with its presumed role as a central mediator of neuroinflammatory response, upregulated within hours of injury^{16,17}. Microglia are themselves suspected to be a major mediator of this early TNF response but our results show a time-dependent decrease in downstream TNF secretion after stimulation with TNF, suggesting an element of negative feedback responsiveness for this particular cytokine. This feedback responsiveness may also fit with the suggestion that TNF appears to function differently in acute versus delayed phases after injury, acting initially as a potent immune mediator but later as a neurotrophic factor required for repair¹⁸. Taken together with our data showing a significantly different panel of downstream cytokine induction in low vs high doses of TNF, a dose-dependent effect of TNF may partially underlie this phenomenon in human tissue and is worthy of further investigation.

The effects of these cytokines on the matrix metalloproteinases, MMP-2 and MMP-9, provides further validation for this approach, as it is consistent with empirical data from the clinical TBI literature. These enzymes are known to undertake tissue remodelling after injury and, in the brain, MMP-9 is thought to be detrimental to recovery, being implicated in expansion of contusional volume and breakdown of the blood-brain barrier^{19,20}. Increased concentrations are found in human pericontusional brain and murine evidence that lesion volumes are reduced with the use of MMP-9 inhibitors after trauma^{21,22}. In contrast, while the evidence for MMP-2 is somewhat mixed, evidence from MMP-2 knockout transgenic

mice suggests MMP-2 as essential for effective wound healing and functional recovery after brain injury²³. Our data suggests microglia cytokine stimulation to be a potent activator of MMP-2 and our previous results from astrocyte cultures appear to preferentially stimulate a MMP-9 response. This fits with the putative role for microglia promoting a more reparative inflammatory network than other glia. In this way one may hypothesise that the MMP-9 response identified in human pericontusional brain is driven by astrocyte responses and that therapeutic strategies directed against this pathway should target astrocytes.

It is notable also that the microglial secretome appears to demonstrate a significant type 1 interferon response, with IFN- α released as a concentration-dependent function of IL-4, IL-10 and TNF. This effect was not apparent in our data from astrocyte or neuronal cultures. A significant type 1 interferon response is known to be mounted in the acute period after brain injury and is emerging as a potential therapeutic target in TBI, as well as other central nervous system diseases with a suspected chronic neuroinflammatory component^{24–27}. Our data supports mouse evidence that microglia are responsible for this interferon response although we highlight recent human transcriptome evidence that oligodendrocytes also mount a significant interferon response after TBI – a cell type that we have not examined in our studies²⁸. These data would support targeting microglia in order to mitigate the type 1 interferon response, in human TBI, but will require further validation in human interventional studies.

The major limitation of our study is the highly reductionist approach we have adopted, using a single cell type with separately applied stimulating cytokines in isolation. This does not capture the complex network of multiple interacting cell and chemokine parts that is at work in-vivo, in particular direct cell-cell interactions. Nevertheless, through this series of studies examining single cell types in turn, we have attempted to build a foundation, specifically in the human context, to begin to unravel the network of inflammatory cytokine signalling that is at work after TBI. These results will provide a platform to enable interpretation of more complex studies and rationalisation of animal experiments. While we have focussed on the soluble mediators released by the microglial cells, this does not in itself reflect the functional characteristics of the microglia. In future studies, we will explore microglia functions such as changes in microglial morphology and phagocytosis. We also recognise that the derivation

of microglia from iPSCs, while providing a reliable and reproducible in-vitro platform, may not faithfully recapitulate the state of microglia found in-vivo, with evidence from human transcriptomic studies that these cells exhibit subtly different expression profile to microglia in both normal and injured cortex^{29,30}. The effects of these differences are unknown but it is clear that the heterogeneity of aged and immune-primed microglia will not be captured by this in-vitro system and may be reflected in how they respond.

Conclusion

Human iPSC-derived microglia generate a broad inflammatory cytokine response in response to exogenous stimulating cytokines at the concentrations seen after human TBI. The response is especially evident after exposure to TNF and there is a mix of both pro- and anti-inflammatory cytokine signalling in response to all five stimulating cytokines that were used. We present a dataset for microglia that complements our previous reductionist datasets from examining astrocyte and neuronal cultures with the same approach. This work, and our series of studies, provides a platform for further investigation to understand the complex neuroinflammatory network initiated after traumatic brain injury in a human context.

Transparency, Rigor and Reproducibility statement

This was a laboratory experimental study and the study plan was not formally pre-registered. All experimental materials were analysed at the same time in a single batch. All equipment and analytical reagents used to perform experimental manipulations and measurements are widely available commercially, as detailed in the methods. Statistical analysis was performed using methods outlined in the text. This report includes documentation of internal replication. All available data from this study has been published (Supplementary File 1). Samples collected as part of the study are available to be used for future research and there are requirements for additional informed consent or regulatory controls. The authors agree to provide the full content of the manuscript on request by contacting Adel Helmy.

Conflicts of interest

The authors have no conflicts of interest to declare.

Author contributions

Conceptualisation and design of study: AEH, YAS, EPT, KPC, RP. Performed experiments: AA, TS. Analysis of data: AA, TS, SK, JT, NMG, CL. First draft of manuscript: SK, AA, TS. All authors critically reviewed and approved the final manuscript for publication.

References

1. James SL, Bannick MS, Montjoy-Venning WC, et al. Global, regional, and national burden of traumatic brain injury and spinal cord injury, 1990-2016: A systematic analysis for the Global Burden of Disease Study 2016. *Lancet Neurol* 2019;18(1):56–87; doi: 10.1016/S1474-4422(18)30415-0.
2. Maas AIR, Menon DK, Manley GT, et al. Traumatic brain injury: progress and challenges in prevention, clinical care, and research. *Lancet Neurol* 2022;21(11):1004–1060; doi: 10.1016/S1474-4422(22)00309-X.
3. Thelin EP, Tajsic T, Zeiler FA, et al. Monitoring the Neuroinflammatory Response Following Acute Brain Injury. *Front Neurol* 2017;0(JUL):351; doi: 10.3389/FNEUR.2017.00351.
4. Simon DW, McGeachy MJ, Baylr H, et al. The far-reaching scope of neuroinflammation after traumatic brain injury. *Nat Rev Neurol* 2017 133 2017;13(3):171–191; doi: 10.1038/nrneurol.2017.13.
5. Salter MW, Stevens B. Microglia emerge as central players in brain disease. *Nat Med* 2017 239 2017;23(9):1018–1027; doi: 10.1038/nm.4397.
6. Loane DJ, Kumar A. Microglia in the TBI brain: The good, the bad, and the dysregulated. *Exp Neurol* 2016;275:316–327; doi: 10.1016/J.EXPNEUROL.2015.08.018.
7. Hammond TR, Dufort C, Dissing-Olesen L, et al. Single-Cell RNA Sequencing of Microglia throughout the Mouse Lifespan and in the Injured Brain Reveals Complex Cell-State Changes. *Immunity* 2019;50(1):253-271.e6; doi: 10.1016/J.IMMUNI.2018.11.004.
8. Izzy S, Liu Q, Fang Z, et al. Time-Dependent Changes in Microglia Transcriptional Networks Following Traumatic Brain Injury. *Front Cell Neurosci* 2019;13:307; doi: 10.3389/FNCEL.2019.00307/BIBTEX.
9. Muffat J, Li Y, Yuan B, et al. Efficient derivation of microglia-like cells from human pluripotent stem cells. *Nat Med* 2016;22(11):1358–1367; doi: 10.1038/NM.4189.

10. Helmy A, Carpenter KLH, Menon DK, et al. The cytokine response to human traumatic brain injury: temporal profiles and evidence for cerebral parenchymal production. *J Cereb Blood Flow Metab* 2011;31(2):658; doi: 10.1038/JCBFM.2010.142.
11. Helmy A, Guilfoyle MR, Carpenter KLH, et al. Recombinant human interleukin-1 receptor antagonist in severe traumatic brain injury: a phase II randomized control trial. *J Cereb Blood Flow Metab* 2014;34(5):845–851; doi: 10.1038/JCBFM.2014.23.
12. Thelin EP, Hall CE, Gupta K, et al. Elucidating Pro-Inflammatory Cytokine Responses after Traumatic Brain Injury in a Human Stem Cell Model. *J Neurotrauma* 2018;35(2):341–352; doi: 10.1089/NEU.2017.5155/ASSET/IMAGES/LARGE/FIGURE4.JPEG.
13. Thelin EP, Hall CE, Tyzack GE, et al. Delineating astrocytic cytokine responses in a human stem cell model of neural trauma. *J Neurotrauma* 2020;37(1):93–105; doi: 10.1089/NEU.2019.6480/SUPPL_FILE/SUPP_FIGS4.PDF.
14. Jassam YN, Izzy S, Whalen M, et al. Neuroimmunology of Traumatic Brain Injury: Time for a Paradigm Shift. *Neuron* 2017;95(6):1246–1265; doi: 10.1016/J.NEURON.2017.07.010.
15. Ramlackhansingh AF, Brooks DJ, Greenwood RJ, et al. Inflammation after trauma: Microglial activation and traumatic brain injury. *Ann Neurol* 2011;70(3):374–383; doi: 10.1002/ANA.22455.
16. Ziebell JM, Morganti-Kossmann MC. Involvement of Pro-and Anti-Inflammatory Cytokines and Chemokines in the Pathophysiology of Traumatic Brain Injury. n.d.
17. Shohami E, Novikov M, Bass R, et al. Closed head injury triggers early production of TNF alpha and IL-6 by brain tissue. *J Cereb Blood Flow Metab* 1994;14(4):615–619; doi: 10.1038/JCBFM.1994.76.
18. Longhi L, Perego C, Ortolano F, et al. Tumor necrosis factor in traumatic brain injury: effects of genetic deletion of p55 or p75 receptor. *J Cereb Blood Flow Metab* 2013;33(8):1182; doi: 10.1038/JCBFM.2013.65.

19. Candelario-Jalil E, Yang Y, Rosenberg GA. Diverse roles of matrix metalloproteinases and tissue inhibitors of metalloproteinases in neuroinflammation and cerebral ischemia. *Neuroscience* 2009;158(3):983–994; doi: 10.1016/J.NEUROSCIENCE.2008.06.025.
20. Vandooren J, Van Den Steen PE, Opdenakker G. Biochemistry and molecular biology of gelatinase B or matrix metalloproteinase-9 (MMP-9): the next decade. *Crit Rev Biochem Mol Biol* 2013;48(3):222–272; doi: 10.3109/10409238.2013.770819.
21. Guilfoyle MR, Carpenter KLH, Helmy A, et al. Matrix Metalloproteinase Expression in Contusional Traumatic Brain Injury: A Paired Microdialysis Study. *J Neurotrauma* 2015;32(20):1553; doi: 10.1089/NEU.2014.3764.
22. Jiang XF, Namura S, Nagata I. Matrix metalloproteinase inhibitor KB-R7785 attenuates brain damage resulting from permanent focal cerebral ischemia in mice. *Neurosci Lett* 2001;305(1):41–44; doi: 10.1016/S0304-3940(01)01800-6.
23. Hsu JYC, McKeon R, Goussev S, et al. Matrix Metalloproteinase-2 Facilitates Wound Healing Events That Promote Functional Recovery after Spinal Cord Injury. *J Neurosci* 2006;26(39):9841–9850; doi: 10.1523/JNEUROSCI.1993-06.2006.
24. Abdullah A, Zhang M, Frugier T, et al. STING-mediated type-I interferons contribute to the neuroinflammatory process and detrimental effects following traumatic brain injury. *J Neuroinflammation* 2018;15(1):1–17; doi: 10.1186/S12974-018-1354-7/FIGURES/10.
25. Barrett JP, Henry RJ, Shirey KA, et al. Interferon- β Plays a Detrimental Role in Experimental Traumatic Brain Injury by Enhancing Neuroinflammation That Drives Chronic Neurodegeneration. *J Neurosci* 2020;40(11):2357; doi: 10.1523/JNEUROSCI.2516-19.2020.
26. Barrett JP, Knobloch SM, Bhattacharya S, et al. Traumatic Brain Injury Induces cGAS Activation and Type I Interferon Signaling in Aged Mice. *Front Immunol* 2021;12:3396; doi: 10.3389/FIMMU.2021.710608/BIBTEX.

27. Wangler LM, Bray CE, Packer JM, et al. Amplified Gliosis and Interferon-Associated Inflammation in the Aging Brain Following Diffuse Traumatic Brain Injury. *J Neurosci* 2022;JN-RM-1377-22; doi: 10.1523/JNEUROSCI.1377-22.2022.
28. Garza R, Sharma Y, Atacho D, et al. Single-cell transcriptomics of resected human traumatic brain injury tissues reveals acute activation of endogenous retroviruses in oligodendrocytes. *bioRxiv* 2022;2022.09.07.506982; doi: 10.1101/2022.09.07.506982.
29. Olah M, Patrick E, Villani AC, et al. A transcriptomic atlas of aged human microglia. *Nat Commun* 2018;9(1); doi: 10.1038/S41467-018-02926-5.
30. Young AMH, Kumasaka N, Calvert F, et al. A map of transcriptional heterogeneity and regulatory variation in human microglia. *Nat Genet* 2021 536 2021;53(6):861–868; doi: 10.1038/s41588-021-00875-2.

Funding statement

AA is supported as Newton International Fellow by the Academy of Medical Sciences and Newton Fund, UK (#NF170920). EPT is supported through the Strategic Research Area Neuroscience (STRATNeuro), The Erling-Persson Foundation, Region Stockholm Clinical Research Appointment (#FoUI-981490) and Karolinska Institutet Research Grants (#2022-01576). KLHC is supported by the NIHR Biomedical Research Centre, Cambridge, by an NIHR i4i Challenge Award II-C5-0715- 20005, an NIHR i4i Product Development Award NIHR200986, and the NIHR Brain Injury MedTech Co-operative. The views expressed are those of the authors and are not necessarily those of the NIHR or the Department of Health and Social Care.

Table 1. Cytokine concentrations used to stimulate the microglial culture (pg mL^{-1})

	IL-1β	IL-10	IL-4	IL-6	TNF
Range seen physiologically	0.02 – 21	0.8 – 173	0.1 – 37	0.15 – 4990	0.05 – 23
Range applied in <i>in vitro</i> conditions:					
Low	1	1	1	100	1
Medium	100	100	100	10000	100
High	10000	10000	10000	1000000	10000

Table 2. Summarizes time and/or concentration dependent alterations in the microglial production of cytokines following stimulation using recombinant cytokines. The “(↑= increase) or (↓= decrease)” indicates that the specific cytokine induction produced a significant increased or decreased concentration of a specific cytokine in that model, whereas “–” indicates no significant changes. The sum of all significant increases or decrease is presented at the bottom.

	TIME					CONCENTRATION					TIME x CONCENTRATION				
	IL-1β	IL-10	IL-4	IL-6	TNF	IL-1β	IL-10	IL-4	IL-6	TNF	IL-1β	IL-10	IL-4	IL-6	TNF
MIP-1α	–	–	–	–	–	–	–	–	–	–	–	–	–	–	–
MMP-9	↓	↓	↓	↓	↑	–	↓	↑	↑	↑	–	↓	–	–	↑
BLC/CXCL13	–	–	↓	–	↓	–	–	–	–	–	–	–	–	–	–
MMP-2	↑	↑	↑	↑	↑	↑	–	↑	–	–	↑	–	↑	–	–
IL-4	↓	–	↓	↓	↑	↑	–	↑	–	↑	–	–	–	–	↑
IL-1β	↓	–	–	–	–	↑	–	–	–	–	–	–	–	–	–
IP-10	–	–	–	–	↑	–	–	–	–	↑	–	–	–	–	↑
IL-6	↓	–	–	↓	↑	↑	↑	–	↑	↑	–	–	–	–	↑
TIMP-1	↑	↑	↑	↑	↑	–	–	–	–	↑	–	–	–	–	↑
IL-8	↑	–	–	–	↑	↑	–	–	↑	↑	↑	–	–	–	↑
IL-10	–	↓	–	–	–	–	↑	–	–	–	–	–	–	–	–
IL-12p70	–	–	–	–	–	–	–	–	–	–	–	–	–	–	–
Eotoxin	–	–	–	–	↑	↑	–	↑	–	↑	–	–	–	–	↑
MDC/CCL22	–	–	↓	–	–	–	–	↑	–	–	–	–	–	–	–
IL-17A	–	–	–	–	–	–	–	–	–	–	–	–	–	–	–
IL-1 RA	–	–	–	–	–	–	–	↑	–	–	–	–	–	–	–
Fractalkine	–	–	–	–	↑	↑	–	–	–	↑	–	–	–	–	↑
RANTES	–	–	–	–	↑	–	–	–	–	↑	–	–	–	–	↑
IFN-γ	–	↑	–	↑	↑	↑	–	↑	–	–	–	–	–	–	–
TNF-α	–	–	–	–	↓	–	–	–	–	–	–	–	–	–	–
TGF-α	–	–	–	–	–	–	–	–	–	–	–	–	–	–	–
MIP-1β	↑	–	–	–	–	–	–	–	–	↑	–	–	–	–	–
IFN-α	–	–	–	–	–	–	↑	↑	–	↑	–	–	–	–	–
MCP-1	↑	↑	↑	↑	↓	↑	–	–	–	↑	↑	–	–	–	–
VEGF-D	–	–	–	–	↑	–	–	–	–	↑	–	–	–	–	↑
MIP-3α	–	–	–	–	–	–	–	–	–	↑	–	–	–	–	–
BDNF	–	–	–	–	–	–	–	–	–	↑	–	–	–	–	–
GRO-α	↑	–	–	–	↑	↑	–	↑	–	–	↑	–	–	–	–
IL-1α	–	–	–	–	↑	↑	–	–	–	↑	–	–	–	–	↑
IL-23	–	–	↓	–	–	–	–	↑	–	–	–	–	–	–	–
BAFF	–	–	–	–	–	–	–	–	–	–	–	–	–	–	–
MCP-3	–	–	–	–	↑	–	–	–	–	↑	–	–	–	–	↑
M-CSF	–	–	–	–	–	–	–	–	–	–	–	–	–	–	–
G-CSF	–	–	–	–	–	–	–	–	–	–	–	–	–	–	–
CD40L	–	–	–	–	–	–	–	–	–	–	–	–	–	–	–
MCP-2	↑	–	–	–	–	–	–	–	–	↑	–	–	–	–	–
VEGF-A	–	–	–	–	↑	–	–	–	–	↑	–	–	–	–	↑
Sum increase	7	4	3	4	16	11	3	10	3	19	4	0	1	0	13
Sum decrease	4	2	5	3	3	0	1	0	0	0	0	1	0	0	0
Sum changes	11	6	8	7	19	11	4	10	3	19	4	1	1	0	13

Table 3. Summary of the downstream cytokine secretion by cytokine-induced neurons, astrocytes and microglia

Cytokine added	Cytokine induced Neurons	Cytokine induced Astrocytes	Cytokine induced Microglia
	Time		
IL-1 β	-	BAFF, TIMP1, MMP9, VEGF-A	TIMP1, MIP1 β , MCP-2
IL-10	-	MMP9, M-CSF	MMP2, TIMP1, IFN γ , MCP1
IL-4	-	MMP9, M-CSF	TIMP1, MCP1
IL-6	IL-1ra, IL-5, IL-13, MIP1 α , RANTES	MMP9	MMP2, TIMP1, IFN- γ , MCP1
TNF	Fractalkine, IL-6, IL-10	MMP9, M-CSF	MMP2, IFN γ , GRO α
	Concentration		
IL-1 β	IP10	IL-1ra, RANTES, IP10, Eotaxin, M-CSF, VEGF-D	IL4, IL-1 β , IL6, Eotaxin, Fractalkine, IFN γ , IL-1 α
IL-10	-	IL-1 α	IL6, IL10, IFN α
IL-4	-	-	MMP9, IL4, Eotaxin, MDC/CCL22, IL-1ra, IFN γ , IFN α , GRO α , IL23
IL-6	IL-1 α , IL-4, sCD40L	sCD40L	MMP9, IL-6, IL-8
TNF	Eotaxin, GM-CSF, IP10	-	MIP1 β , IFN α , MCP1, VEGF-D, MIP-3 α , BDNF, GRO α , IL1 α , MCP3, VEGF-A

	Time × Concentration		
IL-1 β	-	MCP-2, IL-8, MIP-1 α , IL-1 α , GRO α , Fractalkine, MIP1 β	MMP2, IL8, MCP1, GRO α ,
IL-10	-	IL-8, VEGF-A	-
IL-4	-	IL-8, IL-1 α , VEGF-A	MMP2
IL-6	Fractalkine, GM-CSF, IFN α , IFN γ , IL-12p70, MIP1 β , sIL-2Ra, TNF	IL-8, MIP1 α , IL-1 α , TIMP1, VEGF-A, M-CSF	-
TNF	GRO α , IL-1 α , IL-8, MCP3, MIP-1 β , RANTES, sCD40L	IL-8, IL-1 α , VEGF-A, MIP-1 β	MMP9, IL4, IP10, IL6, TIMP1, IL8, Eotaxin, Fractalkine, RANTES, VEGF-D, IL-1 α , MCP3, VEGF-A

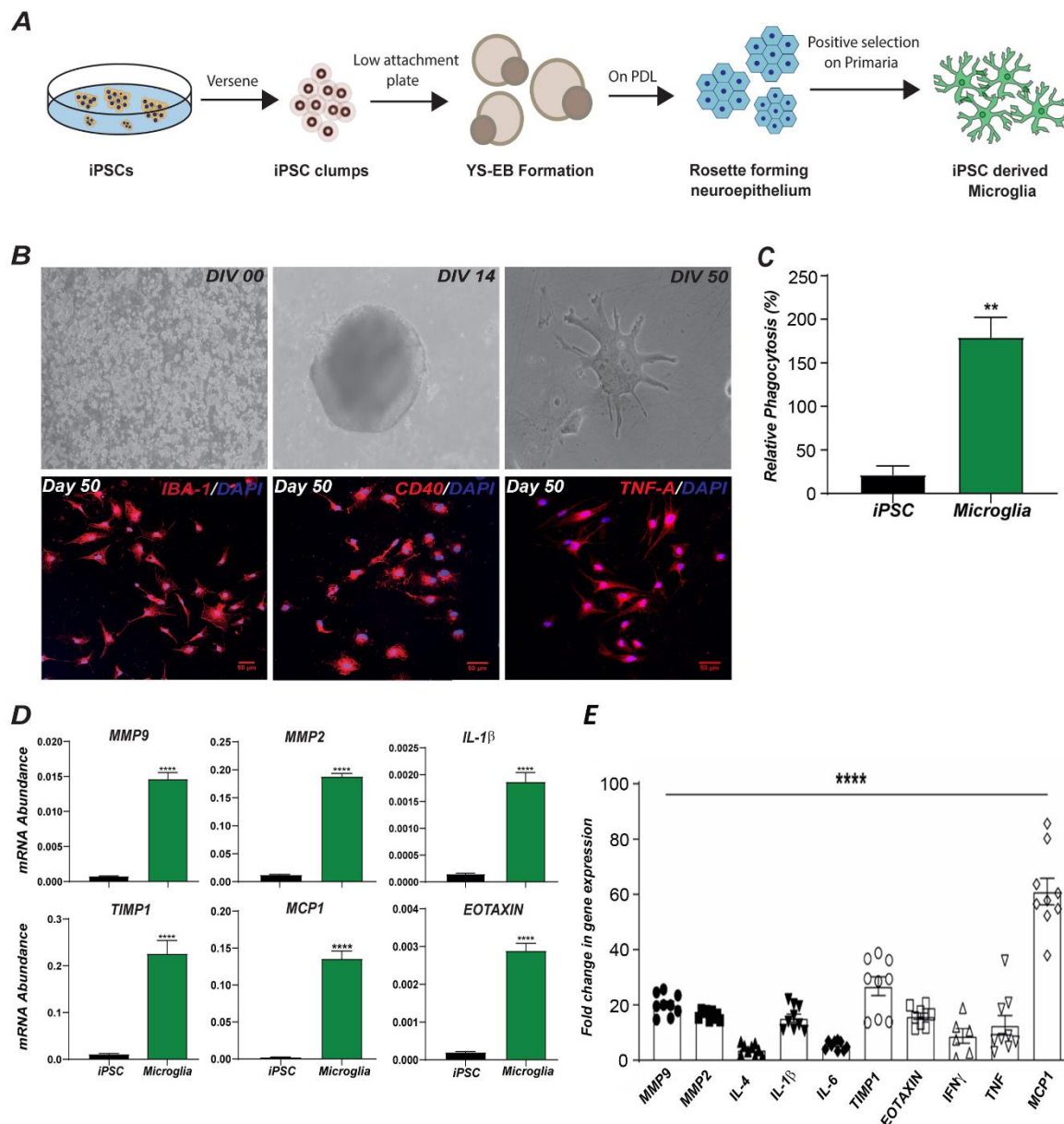


Figure 1 Generation of microglia from human induced pluripotent stem cells

(A) Timeline showing differentiation of microglia from human-derived iPSCs (hiPSCs). hiPSCs were used to generate embryoid bodies using suspension culture, followed by dissociation which led to generation of neuroepithelium on an adherent surface and were further differentiated into mature microglia.

(B) Representative bright field images of microglia. (Top Panel) DIV00 illustrates dissociated hiPSCs on a low attachment plate, DIV14 illustrates an embryoid body in a suspension culture, DIV50 shows mature microglia. Representative fluorescent images of iPSC-derived

mature microglia. (Bottom Panel) Microglia expressing IBA1 (red), CD40 (red) and TNF-A (red), counterstained with DAPI (blue) (scale bar 50 μ m).

(C) Representative bar graph for relative phagocytosis ability of hiPSC-derived microglia in response to 20ng/ml LPS compared unstimulated iPSCs. Data shown as mean \pm SEM * p<0.03, ** p<0.002, *** p<0.0002 and **** p<0.0001 using Unpaired t-test with Welch's correction

(D) mRNA levels of some important microglial markers: MMP-9, MMP-2, IL-1 β , TIMP-1, MCP-1 and Eotaxin in iPSC-derived microglia at Day 50. Data shown as mean \pm SEM * p<0.03, ** p<0.002, *** p<0.0002 and **** p<0.0001 using Unpaired t-test with Welch's correction.

(E) Bar plots illustrating a fold change in gene expression using $2^{-\Delta\Delta CT}$ value comparing unstimulated hiPSCs and microglial cultures. Data shown as mean \pm SEM * p<0.03, ** p<0.002, *** p<0.0002 and **** p<0.0001 using One-Way ANOVA.

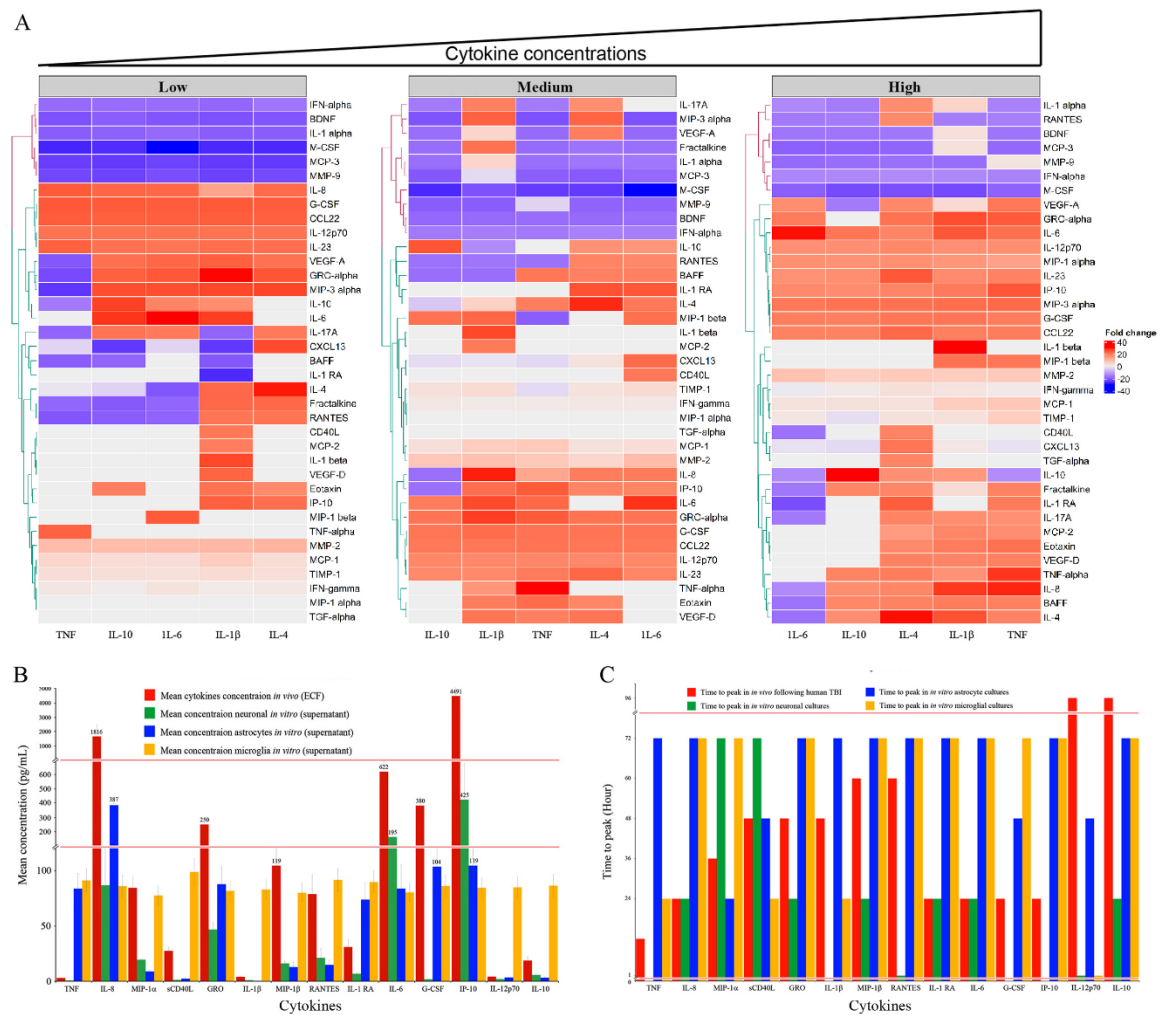


Figure 2. Microglial response to stimulating cytokines

(A) Heatmap showing the change in cytokine secretion by microglia upon cytokine stimulation. Changes in cytokine production are displayed as the absolute value of the fold change, represented on a logarithmic scale. The displayed fold changes correspond to the greatest fold change observed across the four investigated time points. Results corresponding to all the different time points and concentrations of inducing cytokines are shown in **Supplementary Figure 1**.

(B) Mean concentrations of some cytokines released from microglia, astrocytes, and neurons (*in vitro*) along with previously analyzed in the aftermath of human TBI

(C) Comparisons of time to peak of cytokines in *in vivo* human TBI, and in *in vitro* (neuronal, astrocytes, and microglial) models of neuroinflammation. Time to peak describes the highest concentrations that could be seen following either trauma or cytokine induction.